CMS Physics Analysis Summary

Contact: cms-pag-conveners-exotica@cern.ch 2016/08/04

Search for the third-generation scalar leptoquarks and heavy right-handed neutrinos in $\tau_\ell \tau_h$jj final states in pp collisions at 13 TeV

The CMS Collaboration

Abstract

A search is performed for the third-generation scalar leptoquarks and heavy right handed neutrinos in events containing one electron or muon, one hadronically decaying τ lepton, and at least two jets, using a $\sqrt{s} = 13$ TeV pp collision data sample corresponding to 12.9 fb^{-1} collected by the CMS detector at the LHC in 2016. The number of observed events is found to be in agreement with the standard model prediction in both search analyses. A 95% CL limit is set on the product of the leptoquark pair production cross section and β^2, where β is the branching fraction of the leptoquark decay to a τ lepton and a b quark. Assuming $\beta = 1$, the third-generation leptoquarks with masses below 900 GeV are excluded at 95% CL. The right-handed neutrinos are searched in decays of right-handed W_R bosons. The heavy right-handed neutrinos are excluded at 95% CL for a range of neutrino masses below the W_R mass, dependent on the value of M_{W_R}. Assuming the mass of neutrino to be half of the mass of right-handed W boson, W_R boson masses below 3.2 TeV are excluded at 95% CL.

1 Introduction

A number of extensions of the standard model (SM) such as SU(5) grand unified theory [1], SU(4) Pati-Salam [2] and compositeness models [3, 4], superstrings [5], technicolor [6–8] and many other models predict particles, called leptoquarks (LQ), that carry color charge, fractional electric charge, and both lepton and baryon quantum numbers. The LQ may decay to a lepton and a quark. Stringent limits on flavour changing neutral currents [9] indicate that leptoquarks decay predominantly to a lepton and a quark from the same generation [4, 9–12].

The branching fraction, β, of a leptoquark decay to a quark and a charged lepton is model dependent. The rate of pair production of scalar leptoquarks is determined by the strong interactions, and the only free parameter is the mass of the LQ. In particular, the production of LQ pairs is independent of the coupling of the LQ to a lepton and quark, λ. The dominant production mechanisms at the LHC are gluon-gluon fusion and quark-quark annihilation, resulting in a large production cross section.

Here we present a search for the pair production of third generation scalar leptoquarks using 13 TeV pp collision data equivalent to an integrated luminosity of 12.9 fb^{-1} in 2016. Each leptoquark decays to a τ lepton and a b quark. We focus on signatures with one of the τ leptons decaying to an electron or a muon, referred to as light lepton (τ_ℓ) in the following, and the other τ lepton decaying hadronically, denoted by τ_h. In addition, events must contain at least two jets, one of which must be originating from the hadronization of a b quark.

The observation of neutrino oscillation [13] implies that neutrinos have mass, and the fact that the neutrino mass scale is far below the mass of quarks and charged leptons suggests that the mechanism responsible for neutrino masses could be different from that of SM electrically charged fermions. This fact is often considered as evidence of physics beyond the SM, and several models have been proposed to explain this phenomenon. One of the attractive features of left-right (L-R) symmetric extensions [14] to the SM is that these models predict existence of heavy charged (W_R) and neutral (Z_R) gauge bosons that could be produced at LHC energies. The heavy neutrinos (N_e, N_μ, N_τ) naturally arise as the right-handed (RH) partners of the SM neutrinos in these L-R extensions through the see-saw mechanism [15]. Thus, a TeV-scale L-R symmetric theory provides an attractive class of see-saw models that can be probed at the LHC [16].

In this analysis, we also search for heavy right-handed neutrinos produced from the decay of the W_R bosons, $W_R \to \tau + N_\tau$, where $N_\tau \to \tau + W_R \to \tau + q + q$. The final state consists of two τ leptons and at least two jets from hadronization of quarks. Similarly to the LQ3 search, we focus on signatures with one τ_ℓ, one τ_h, and at least two more jets. The search for RH neutrinos is carried out in the $e\tau_\text{h}$ and $\mu\tau_\text{h}$ channels.

Previous searches for third generation leptoquarks were carried out at pp, $\text{p}\bar{\text{p}}$, e^+e^-, and ep colliders (see [17] and references therein). The most stringent lower limit on the mass of scalar third generation leptoquarks to date, in the final state with two τ leptons and two b-jets and assuming $\beta = 1$, is at $\sim$740 GeV from the CMS experiments [18, 19]. Previous searches for heavy neutrino and right-handed W have been performed in di-electron and di-muon channel excluding the W_R with masses up to 3 TeV [20]. Using 13 TeV pp collision data collected in 2015, the CMS experiment searched for heavy neutrino and right-handed W using events in which both τ leptons decay hadronically, excluding W_R with masses below 2.35 (1.63) TeV at a 95% confidence level (CL), assuming the N_τ mass is 0.8 (0.2) times the mass of W_R boson [19].

2 The CMS detector

The central feature of the CMS apparatus is a superconducting solenoid of 6 m internal diameter, providing a magnetic field of 3.8 T. Within the solenoid volume are a silicon pixel and strip tracker, a lead tungstate crystal electromagnetic calorimeter (ECAL), and a brass and scintillator hadron calorimeter (HCAL), each composed of a barrel and two endcap sections. Muons are detected in gas-ionisation detectors embedded in the steel flux-return yoke outside the solenoid. Extensive forward calorimetry complements the coverage provided by the barrel and endcap detectors. A detailed description of the CMS detector, together with a definition of the coordinate system used and the relevant kinematic variables, can be found in Ref. [21].

The first level of the CMS triggering system (Level-1), composed of custom hardware processors, uses information from the calorimeters and the muons detectors to select the most interesting events in a fixed time interval of less than 4 μs. The high-level trigger (HLT) processor farm further decreases the event rate from around 100 kHz to less than 1 kHz, before data storage.

3 Event reconstruction and selection

Objects are reconstructed using the particle-flow (PF) algorithm [22], which exploits information from all subdetectors to identify individual particles, such as charged hadrons, neutral hadrons, muons, electrons and photons. Complex objects, such as τ_h, jets, and missing transverse energy ($E_{\mathrm{T}}^{\mathrm{miss}}$), are reconstructed from these individual particles. The reconstructed interaction vertex with the largest value of $\sum_i p_T^i$, where p_T^i is the transverse momentum of the i^{th} track associated with the vertex, is selected as the primary event vertex. This vertex is used as the reference vertex for all the objects reconstructed using the PF algorithm.

Electrons are reconstructed by matching ECAL superclusters to tracks reconstructed in the silicon pixel and strip detectors. The electrons selected in this analysis are required to have transverse momenta $p_T > 50\,\mathrm{GeV}$ and $|\eta| < 2.1$. The identification and isolation of electron is based on the multivariate technique [23] and selected electrons must satisfy tight electron identification and isolation criteria.

Muon reconstruction starts by matching tracks in the silicon tracker with tracks in the outer muon spectrometer [24]. A global muon track is fitted to the hits from both tracks. Muons are required to satisfy the conditions $p_T > 50\,\mathrm{GeV}$ and $|\eta| < 2.1$. Quality criteria are applied on the muon tracks to distinguish genuine muons from muons coming from cosmic rays. In addition, muons are required to pass isolation criteria to separate prompt muons from those associated with a jet, usually from the semi-leptonic decays of heavy quarks, and must be isolated from other particles in the event.

The hadron-plus-strips (HPS) algorithm [25, 26] is used to reconstruct the τ_{h} candidates. It starts from a jet, and searches for candidates produced by the main τ_h decay modes of the τ lepton: either directly to one charged hadron, or via intermediate ρ and $\mathrm{a}_1(1280)$ mesons to one charged hadron plus one or two neutral pions, or three charged hadrons. The reconstructed τ_{h} is required to have $|\eta| < 2.3$ and $p_T > 50\,\mathrm{GeV}$ ($p_T > 60\,\mathrm{GeV}$) in the LQ (RH heavy neutrino) search. Tau isolation computation is based on a multivariate technique exploiting the tau decay lifetime information. Loose working of the tau isolation has been used which corresponds to the approximately 65% tau identification efficiency and less than 1% jet to tau mis identification rate. Additional criteria are applied to discriminate against electrons and muons reconstructed as τ_{h} candidates.

The identified electron (muon) and τ_h are required to originate from the same vertex and be separated spatially by $\Delta R \equiv \sqrt{\Delta\phi^2 + \Delta\eta^2} > 0.5$. Events containing additional electrons or muons of $p_T > 15\,\text{GeV}$, passing loose identification and isolation criteria, are vetoed.

Jets are reconstructed with the anti-k_t algorithm with a size parameter R = 0.4 [27, 28] using PF candidates. Jet energy is corrected for the average contribution from particles from other proton-proton collisions in the same bunch crossing (pileup). Additional correction is applied to better reflect the true total momentum of the particles in the jet [29]. Selected jets are required to be within $|\eta| < 2.4$ and have $p_T > 50\,\text{GeV}$, and to be separated from the selected electron or muon and the τ_h by $\Delta R > 0.5$.

The transverse momentum imbalance, E_T^{miss}, is calculated as a negative vectorial sum of all particle-flow candidates. To improve its response, E_T^{miss} is corrected by propagating the corrections applied to identified jets. A correction is applied to account for the effect of additional pileup interactions. In addition several filters have been deployed to veto events with large E_T^{miss} caused by detector effects.

Candidate events were collected using a set of triggers requiring the presence of either an electron or a muon with transverse momentum thresholds of 45 GeV.

The search for leptoquarks is performed in a sample of events containing one light lepton a hadronically decaying tau, and at least two jets, with at least one of the two leading jets identified as originating from b quark hadronization (b-tagged) using the combined secondary vertex (CSV) algorithm [30]. The lepton and the τ_h are also required to have opposite electric charge. Additionally, the mass of the τ_h and a jet ($M(\tau_h, j)$) is required to be greater than 250 GeV. Among the two possible jets, the one is paired with τ_h which minimises the difference between the mass of the τ_h and one jet and the mass of the lepton and the other jet.

The search for W_R decaying to a heavy neutrino is performed in a sample of events containing one light lepton (electron or muon for $e\tau_h$ and $\mu\tau_h$ channels, respectively), a hadronically decaying tau, and at least two jets. The E_T^{miss} is required to be above 50 GeV and the invariant mass of the light lepton and the τ_h is required to be greater than 150 GeV.

In leptoquark analysis, signal efficiency ranges between 1 to 5% for masses between 300 GeV to 1500 GeV, respectively and in W_R analysis signal efficiency varies between 2 to 7% for masses between 1 to 4 TeV, respectively.

The S_T distribution after the final selection is used to to search for a possible excess of events with respect to the background that could indicate the presence of signal. S_T is defined as the scalar sum of transverse momentum of all required final state objects as well as missing transverse energy.

$$S_T = p_T(\ell) + p_T(\tau_h) + p_T(jet_1) + p_T(jet_2) + E_T^{miss} \quad (1)$$

4 Background estimation

Several standard model processes can mimic the final state signatures explored in this search. The $t\bar{t}$ production is the dominant background due to the presence of the genuine leptons, E_T^{miss} and both light and heavy flavour jets. Additionally, the production of a W or Z boson in association with jets, diboson, single top, and the QCD multijet production can also contribute to the considered final state.

Background and signal processes are modelled using the following simulated samples. The PYTHIA v8.2 generator [31] is used to model the signal and diboson processes. The leptoquark signal samples are generated with masses ranging from 250 GeV to 1500 GeV in steps of 50 GeV in LQ mass. The branching ratio of the LQ to τ lepton and b quark is assumed to be 100%. The W_R signal samples are generated with masses ranging from 1000 GeV to 3000 GeV in steps of 500 GeV in mass of the W_R boson. The mass of the heavy neutrino is assumed to be half of the W_R mass. The MADGRAPH_AMC@NLO generator [32] is used to model the $t\bar{t}$, W+jets, Z+jets, and diboson (WW, WZ and Z Z) processes. The single top production is modeled with the POWHEG [33] generator. Both MADGRAPH_AMC@NLO and POWHEG generators are interfaced with PYTHIA v8.2 for hadronization and showering. The TAUOLA program [34] is used for τ lepton decay. The signal and background samples are normalized to the next-to-next-to-leading-order (NNLO) and the next-to-leading-order (NLO) cross sections [35, 36], respectively. Small differences between data and MC simulation in trigger, particle identification and isolation efficiencies, and in the resolution of the p_T of jets and $E_{\mathrm{T}}^{\mathrm{miss}}$ are corrected by applying suitably chosen scale factors to simulated events.

The $t\bar{t}$ events in simulation are reweighted according to the top quark p_{T} measured in data [37, 38]. The normalization and shape of the $t\bar{t}$ background is then verified in data sample that consists of events containing an electron, a muon, and at least two jets and including all final selection requirements. Purity of $t\bar{t}$ events in this sample is above 95%. Signal contamination in this control region is found to be negligible and does not affect the data to MC simulation comparison even at the tail of the S_{T} distribution. The normalization and shape of $t\bar{t}$ simulated sample agrees well with the one observed in data. Thus, the MC simulation is used to predict $t\bar{t}$ background in signal region.

The W+jets background mainly arises from events with a genuine electron or muon from the leptonic decay of a W boson and an initial or final state radiation jet misidentified as τ_{h}. The normalisation and shape of W background are obtained from MC simulation and a correction factor is applied on the normalisation to take into account the possible difference between data and MC simulation. The correction factor is estimated in a data sample that consists of $\mathrm{W} \to \mu\nu$ events with three or more associated jets. One of the jets is required to pass τ_{h} identification criteria. Events containing jets which pass the b-tagging criteria are rejected to reduce the contamination from $t\bar{t}$ background. Signal contamination in this control region is negligible. A normalization correction factor for the W background is obtained by performing a binned maximum likelihood fit to the transverse mass distribution of the muon and $E_{\mathrm{T}}^{\mathrm{miss}}$. Transverse mass distribution is found to have the most discriminating power of W background against the other backgrounds. As the input to the fit, the normalisation and shape of all backgrounds are estimated from MC simulation. The uncertainties on the cross section of backgrounds are included as the nuisance parameters to the fit. The contribution from QCD multijet background in the W control region in $\mu\tau_{\mathrm{h}}$ channel is small and derived from MC simulation. The best fit value for the W normalization correction factor is found to be 1.0 ± 0.2. The same scale factor is used for $e\tau_{\mathrm{h}}$ channel as the two channels mainly differ by lepton flavour which is well modelled both in data and MC simulation. Consistency of W scale factor in $e\tau_{\mathrm{h}}$ channel with $\mu\tau_{\mathrm{h}}$ channel has been tested by repeating the above procedure, this time replacing muon with electron. The only difference is that QCD shape is derived from data after inverting the electron identification and isolation and subtracting small contamination of other backgrounds. The measured correction factor in $e\tau_{\mathrm{h}}$ channel is found to be 1.3 ± 0.3 which is consistent with the scale factor derived in the $\mu\tau_{\mathrm{h}}$ channel. A 30% uncertainty is applied on both channels.

The QCD multijet production does not constitute a major background in this search. However, as this background is not well modelled by the MC simulation its contribution in both $\mu\tau_{\mathrm{h}}$ and

$e\tau_{\mathrm{h}}$ channels is estimated from data. This data sample, enriched in QCD multijet background, is selected by inverting the τ_h identification criteria. Events in this data sample are required to pass all criteria of final selection except one: the τ_{h} candidate is required to pass loose, but to fail tight isolation criteria. These events are weighted by the p_{T}-dependent probability of a jet satisfying a loose isolation criteria that will also pass final τ_{h} isolation criteria. This probability is measured as a function of jet p_{T} in an independent data sample for each channel, where lepton is required to fail the isolation and have the same electric charge as τ_{h}.

Other minor backgrounds, arising from the single top, Z boson, and dibosons production are estimated from MC simulation.

5 Systematic uncertainties

The results of the analysis are extracted from a binned fit of the S_{T} distributions in the $e\tau_{\mathrm{h}}$ and $\mu\tau_{\mathrm{h}}$ channels. Systematic uncertainties may affect the normalisation or the shape of the S_{T} distribution of the signal and background processes.

Uncertainties that affect the normalisation of the signal and most of the simulated backgrounds are summarised in Table 1. The uncertainty on the integrated luminosity of the analyzed dataset, amounting to 6.2% [39], affects the normalization of the signal and most of the background processes. Uncertainties in muon and electron identification and trigger efficiency, as well as in the τ_{h} identification efficiency, are determined using the "tag-and-probe" technique [25, 26, 40] and amount 2% for electrons and muons and 6% for τ_{h}. Changes in acceptance due to the uncertainty in the b tagging efficiency and the b mistag rate is measured to be between 3 to 5% depending on the processes. The uncertainty on the yield of QCD multijet and W+jet backgrounds amounts to 30%. The uncertainty on the normalization of the $\mathrm{t\bar{t}}$ background due to the PDF and scale uncertainty amounts to 5% [41, 42]. A 10% uncertainty is attributed to Z boson background while the uncertainty on the diboson and single top background amounts to 15% [43]. The uncertainty in the signal acceptance due to the PDF set included in the simulated samples is evaluated, in accordance to the PDF4LHC recommendations [42, 44] by comparing the results obtained using the CTEQ6.6L, MSTW08, and NNPDF10 PDF sets [45–47] with those from the default PDF set (CTEQ6L1). It amounts to 5% [19].

The energy scales (ES) of τ_{h} and jet affect the shape of S_{T} as well as the normalization of signal and background processes. The effects of ES uncertainties on the analysis are estimated by varying the τ_h and jet energies within their respective uncertainties and recomputing S_{T} after the final selection. The uncertainty on the τ_h ES amounts to 3% [26]. An additional uncertainty of $20\% \cdot pT/1TeV$ is applied to cover the extrapolation from low p_T, where the τ_{h} ES is measured, to high p_T. The uncertainty on the jet energy scale affects the p_T spectrum of the jets and consequently $E_{\mathrm{T}}^{\mathrm{miss}}$ which affects the acceptance as well as the S_{T} distribution, and is applied for all backgrounds where normalization is taken from simulation [48]. The uncertainty on the $E_{\mathrm{T}}^{\mathrm{miss}}$ energy scale affects the acceptance in $\mathrm{W_R} \rightarrow \tau + N_\tau$ analysis as well as the S_{T} distribution in both analyses. These uncertainties are derived by varying the energy scale of the jet and underlying events and is applied for all backgrounds where normalization is taken from simulation. As this uncertainty is found to have negligible effect on the shape, it is considered as a normalisation systematics.

Uncertainty due to the top quark p_T reweighting correction is derived by changing the event weight between zero and twice the nominal reweighting correction. value [37, 38]. Finally, uncertainties due to the limited number of simulated events, or the number of events in the control regions in data, are taken into account. These uncertainties are uncorrelated across

the bins in each background distribution [49]. The systematic uncertainties are represented by nuissance parameters in the fit. Those uncertainties marked with * in the Table 1 are treated correlated between $\mu\tau_{\mathrm{h}}$ and $e\tau_{\mathrm{h}}$ channels.

Table 1: Systematic uncertainties. Those uncertainties marked with * are treated correlated between $\mu\tau_{\mathrm{h}}$ and $e\tau_{\mathrm{h}}$ channels.

	Systematic Source	Uncertainty	
		$\mu\tau_h$	$e\tau_h$
Normalisation	Luminosity *	6.2%	6.2%
	Electron Id	-	2%
	Electron Trigger	-	5%
	Muon Id	2%	-
	Muon Trigger	5%	-
	Tau Id	6%	6%
	b-tagging efficiency/mistag rate *	3-5%	3-5%
	$Z/\gamma* \to ll$ normalization *	10%	10%
	QCD multijet normalisation *	30%	30%
	W+jets normalisation *	30%	30%
	$\mathrm{t\bar{t}}$ cross section (PDF+scale) *	5%	5%
	Diboson cross section *	15%	15%
	Single top quark cross section *	15%	15%
	$E_{\mathrm{T}}^{\mathrm{miss}}$ energy scale *	5%	5%
Shape	Tau energy scale	described in the text	described in the text
	Jet energy scale *	described in the text	described in the text
	$\mathrm{t\bar{t}}$ p_T reweighting *	described in the text	described in the text
	High p_T τ_{h}	described in the text	described in the text

6 Results

The S_{T} distributions in the $e\tau_{\mathrm{h}}$ and $\mu\tau_{\mathrm{h}}$ channels are shown in Fig. 1 for LQ analysis and $\mathrm{W_R} \to \tau + N_\tau$ analysis. No excess is seen above the SM expectation within the statistical and systematical uncertainties in both analyses.

Upper limits on the product of signal cross section times branching ratio are set at 95% confidence level (CL) using the modified frequentist construction CL_s [50]. The limit obtained from the combination of $e\tau_{\mathrm{h}}$ and $\mu\tau_{\mathrm{h}}$ channels is shown in Fig. 2 for LQ analysis and in Fig. 3 for $\mathrm{W_R} \to \tau + N_\tau$ analysis. The observed(expected) limit at 95% CL on the masses of third-generation scalar leptoquarks is set to 900(950) GeV, respectively, assuming a 100% branching fraction for the leptoquark decay to a τ lepton and a b quark. In the heavy right handed neutrino analysis, considering $\mathrm{W_R} \to \tau\mathrm{N}_\ell$ regions in the ($\mathrm{W_R}$,N_ℓ) mass space, and assuming the mass of neutrino to be half of the mass of W boson, the observed(expected) limit at 95% CL on the masses of W boson is set to (3.2) 3.2 TeV, respectively.

7 Conclusion

A search is performed for third generation scalar leptoquarks and for heavy right handed neutrinos in events containing one electron or muon, one hadronically decaying τ lepton, and two or more jets, using a pp collision data at $\sqrt{s} = 13$ TeV centre-of-mass energy recorded by

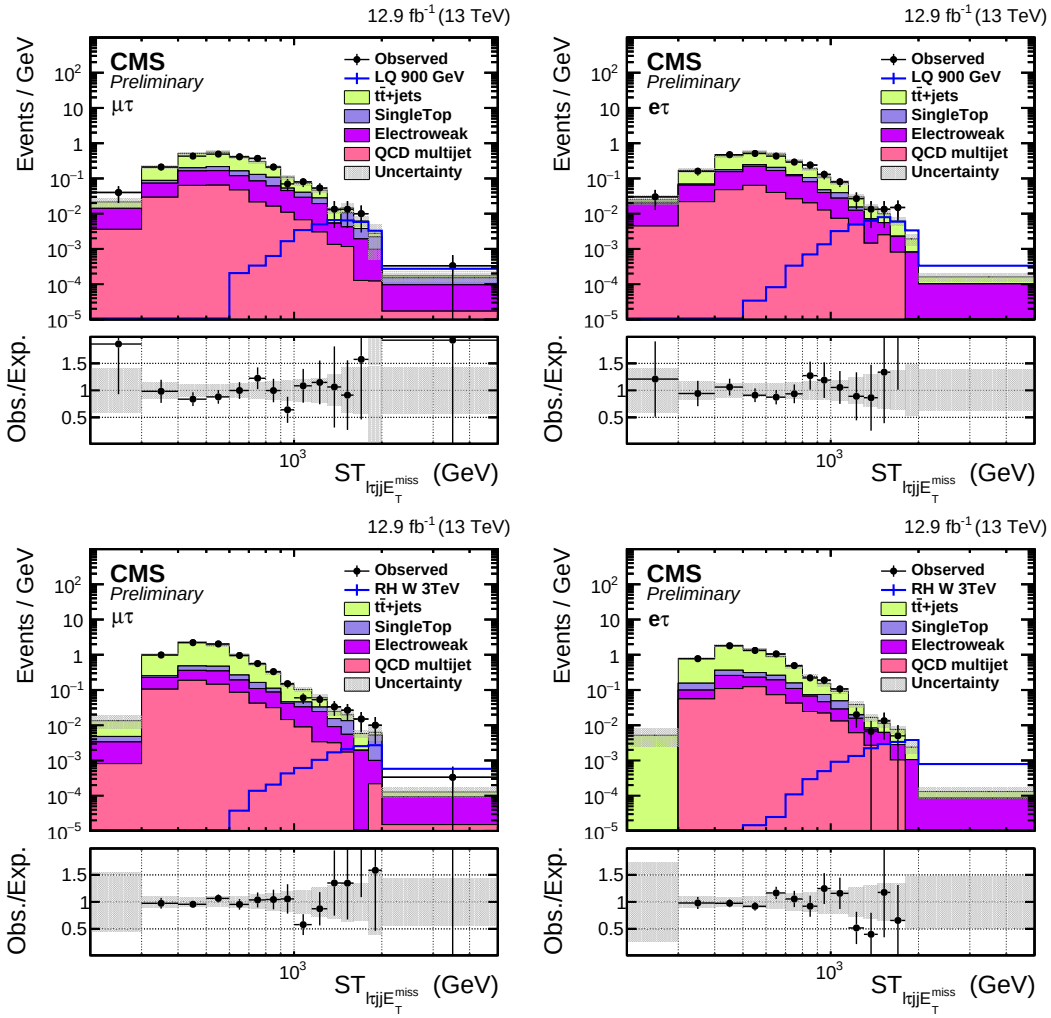

Figure 1: Distribution in S_{T} observed in the $\mu\tau_{\mathrm{h}}$ (left) and $e\tau_{\mathrm{h}}$ (right) channel of the LQ (top) and heavy RH neutrino (bottom) analysis, compared to the expected SM background contribution and to a hypothetic LQ signal of mass $m_{LQ} = 900$ GeV and a hypothetic heavy RH neutrino signal of mass $m_{\mathrm{W_R}} = 3$ TeV. A binned maximum likelihood fit is performed to the S_{T} distribution. "Electroweak" background is the sum of W boson, Z boson, and dibosons. The uncertainty bands represent the sum of statistical and systematic uncertainties, added in quadrature.

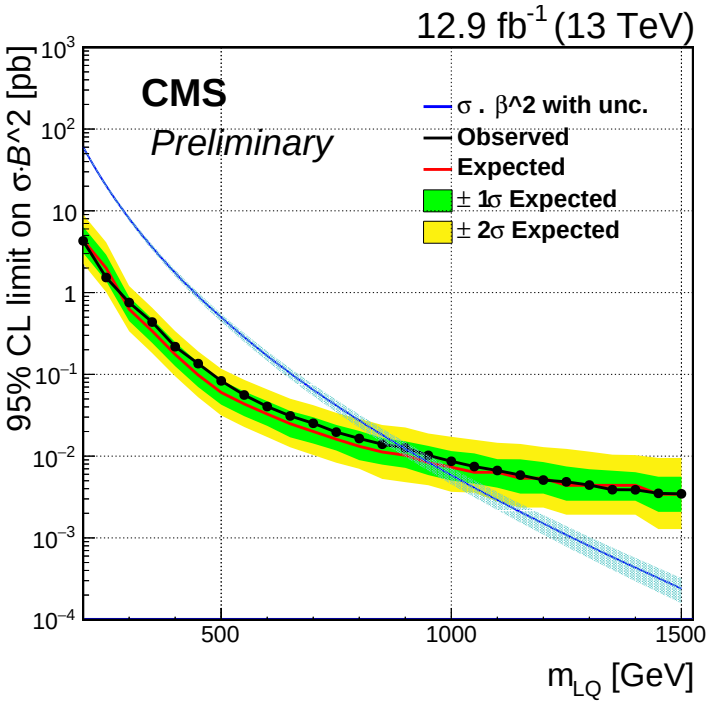

Figure 2: Observed and expected 95% CL upper limit on the product of signal cross section times branching fraction, obtained from the combination of $e\tau_h$ and $\mu\tau_h$ channels, in the LQ analysis. The 1σ and 2σ bands represent the 1 and 2 standard deviation uncertainties on the expected limits.

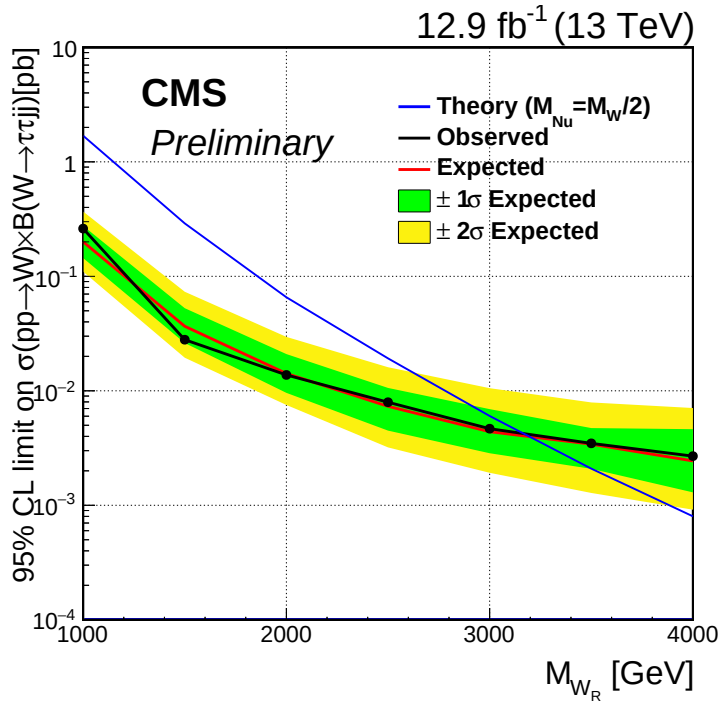

Figure 3: Observed and expected upper limits at 95% CL on the product of cross section and branching fraction for combined $e\tau$ and $\mu\tau$ in heavy right handed neutrino analysis. The 1σ and 2σ bands represent the 1 and 2 standard deviation uncertainties on the expected limits.

the CMS detector at the LHC and corresponding to an integrated luminosity of 12.9 fb^{-1}. The events observed in data is found to be in good agreement with the SM prediction in both search analyses. A 95% CL limit is set on the product of the leptoquark pair production cross section and β^2, where β denotes the branching fraction of decay of the leptoquark to a τ lepton and a b quark. Assuming $\beta = 1$, third generation leptoquarks with masses below 900 GeV are excluded at 95% CL. In the heavy RH neutrino analysis, considering $W_R \to \tau N_\ell$ decay and assuming the mass of heavy neutrino to be half of the mass of W_R boson W boson masses below 3.2 TeV are excluded at 95% confidence level. These results improve the limits from the previous searches for third generation leptoquarks and heavy right handed neutrino with τ lepton in final state.

References

[1] H. Georgi and S. L. Glashow, "Unity of All Elementary Particle Forces", *Phys. Rev. Lett.* **32** (1974) 438, doi:10.1103/PhysRevLett.32.438.

[2] J. C. Pati and A. Salam, "Lepton Number as the Fourth Color", *Phys. Rev. D* **10** (1974) 275, doi:10.1103/PhysRevD.10.275,10.1103/PhysRevD.11.703.2. [Erratum: Phys. Rev.D11,703(1975)].

[3] B. Schrempp and F. Schrempp, "Light leptoquarks", *Phys. Lett. B* **153** (1985) 101, doi:10.1016/0370-2693(85)91450-9.

[4] W. Buchmüller, R. Rückl, and D. Wyler, "Leptoquarks in lepton-quark collisions", *Phys. Lett. B* **191** (1987) 442, doi:http://dx.doi.org/10.1016/0370-2693(87)90637-X.

[5] J. L. Hewett and T. G. Rizzo, "Low-energy phenomenology of superstring-inspired E6 models", *Phys. Rep.* **183** (1989) 193, doi:http://dx.doi.org/10.1016/0370-1573(89)90071-9.

[6] S. Dimopoulos and L. Susskind, "Mass without scalars", *Nucl. Phys. B* **155** (1979) 237, doi:http://dx.doi.org/10.1016/0550-3213(79)90364-X.

[7] S. Dimopoulos, "Technicoloured signatures", *Nucl. Phys. B* **168** (1980) 69, doi:http://dx.doi.org/10.1016/0550-3213(80)90277-1.

[8] E. Eichten and K. Lane, "Dynamical breaking of weak interaction symmetries", *Phys. Lett. B* **90** (1980) 125, doi:http://dx.doi.org/10.1016/0370-2693(80)90065-9.

[9] M. Leurer, "Comprehensive study of leptoquark bounds", *Phys. Rev. D* **49** (Jan, 1994) 333–342, doi:10.1103/PhysRevD.49.333.

[10] O. Shanker, "pl3, kl3, and k0-k0bar constraints on leptoquarks and supersymmetric particles", *Nucl. Phys.* **B 204** (1982) 375.

[11] B. Gripaios, A. Papaefstathiou, K. Sakurai, and W. B., "Searching for third-generation composite leptoquarks at the LHC", arXiv:1010.3962.

[12] C. Amsler et al., "Review of Particle Physics", *Journal of Physics G* **33** (2006) 1+.

[13] W. M. Alberico and S. M. Bilenky, "Neutrino oscillations, masses and mixing", *Phys. Part. Nucl.* **35** (2004) 297–323, arXiv:hep-ph/0306239. [Fiz. Elem. Chast. Atom. Yadra35,545(2004)].

[14] R. N. Mohapatra and J. C. Pati, "A Natural Left-Right Symmetry", *Phys. Rev.* **D11** (1975) 2558, doi:10.1103/PhysRevD.11.2558.

[15] W.-Y. Keung and G. Senjanovic, "Majorana Neutrinos and the Production of the Right-handed Charged Gauge Boson", *Phys. Rev. Lett.* **50** (1983) 1427, doi:10.1103/PhysRevLett.50.1427.

[16] R. N. Mohapatra and G. Senjanovic, "Neutrino Mass and Spontaneous Parity Violation", *Phys. Rev. Lett.* **44** (1980) 912, doi:10.1103/PhysRevLett.44.912.

[17] C. Collaboration, "Search for pair production of third-generation scalar leptoquarks and top quarks in proton-proton collisions at $\sqrt{s} = 8$ TeV", *Physics Letters B* **739** (2014) 229, arXiv:1408.0806.

[18] CMS Collaboration, "Search for pair production of third generation leptoquarks and stops that decay to a tau and a b quark", CMS Physics Analysis Summary CMS-PAS-EXO-12-002, 2012.

[19] CMS Collaboration Collaboration, "Search for heavy neutrinos and third-generation leptoquarks in final states with two hadronically decaying τ leptons and two jets in proton-proton collisions at $\sqrt{s} = 13$ TeV", Technical Report CMS-PAS-EXO-16-016, CERN, Geneva, 2016.

[20] CMS Collaboration, "Search for heavy neutrinos and W bosons with right-handed couplings in proton-proton collisions at $\sqrt{s} = 8$ TeV", *Eur. Phys. J.* **C74** (2014), no. 11, 3149, doi:10.1140/epjc/s10052-014-3149-z, arXiv:1407.3683.

[21] CMS Collaboration, "The CMS experiment at the CERN LHC", *JINST* **3** (2008) S08004, doi:10.1088/1748-0221/3/08/S08004.

[22] CMS Collaboration, "Particle–Flow Event Reconstruction in CMS and Performance for Jets, Taus, and $E_{\mathrm{T}}^{\mathrm{miss}}$", CMS Physics Analysis Summary CMS-PAS-PFT-09-001, 2009.

[23] H. Voss, A. Höcker, J. Stelzer, and F. Tegenfeldt, "TMVA, the toolkit for multivariate data analysis with ROOT", in *XIth International Workshop on Advanced Computing and Analysis Techniques in Physics Research (ACAT)*, p. 40. 2007. arXiv:physics/0703039.

[24] CMS Collaboration, "Performance of CMS muon reconstruction in pp collision events at $\sqrt{s} = 7$ TeV", *JINST* **7** (2012) P10002, doi:10.1088/1748-0221/7/10/P10002, arXiv:1206.4071.

[25] CMS Collaboration, "Performance of tau-lepton reconstruction and identification in CMS", *JINST* **7** (2012) P01001, doi:10.1088/1748-0221/7/01/P01001, arXiv:1109.6034.

[26] CMS Collaboration, "Reconstruction and identification of τ lepton decays to hadrons and ν_τ at CMS", *JINST* **11** (2016), no. 01, P01019, doi:10.1088/1748-0221/11/01/P01019, arXiv:1510.07488.

[27] G. P. Salam, "Towards Jetography", *Eur. Phys. J.* **C67** (2010) 637–686, doi:10.1140/epjc/s10052-010-1314-6.

[28] M. Cacciari, G. P. Salam, and G. Soyez, "The anti-k_t jet clustering algorithm", *JHEP* **04** (2008) 063, doi:10.1088/1126-6708/2008/04/063, arXiv:0802.1189.

[29] CMS Collaboration, "Jet energy scale and resolution in the CMS experiment", CMS Physics Analysis Summary CMS-PAS-JME-13-004, 2013.

[30] CMS Collaboration, "Identification of b-quark jets with the CMS experiment", *JINST* **8** (2013) P04013, doi:10.1088/1748-0221/8/04/P04013, arXiv:1211.4462.

[31] T. Sjöstrand et al., "An introduction to PYTHIA 8.2", *Comput. Phys. Commun* **191** (2014) 159–177, doi:10.1016/j.cpc.2015.01.024, arXiv:1410.3012.

[32] J. Alwall *et al.*, "The automated computation of tree-level and next-to-leading order differential cross sections, and their matching to parton shower simulations", *JHEP* **07** (2014) 079, doi:10.1007/JHEP07(2014)079, arXiv:1405.0301.

[33] C. Oleari, "The POWHEG-BOX", *Nucl. Phys. Proc. Suppl.* **205-206** (2010) 36, doi:10.1016/j.nuclphysbps.2010.08.016, arXiv:1007.3893.

[34] Z. Wąs, "TAUOLA the library for tau lepton decay, and KKMC/KORALB/KORALZ... status report", *Nucl. Phys. B, Proc. Suppl.* **98** (2001) 96, doi:10.1016/S0920-5632(01)01200-2.

[35] M. Kramer, T. Plehn, M. Spira, and P. M. Zerwas, "Pair production of scalar leptoquarks at the CERN LHC", *Phys. Rev.* **D71** (2005) 057503, doi:10.1103/PhysRevD.71.057503, arXiv:hep-ph/0411038.

[36] M. Kramer, T. Plehn, M. Spira, and P. M. Zerwas, "Pair production of scalar leptoquarks at the Tevatron", *Phys. Rev. Lett.* **79** (1997) 341–344, doi:10.1103/PhysRevLett.79.341, arXiv:hep-ph/9704322.

[37] CMS Collaboration, "Measurement of the differential cross section for top quark pair production in pp collisions at $\sqrt{s} = 8$ TeV", *Eur. Phys. J. C* **75** (2015), no. 11, 542, doi:10.1140/epjc/s10052-015-3709-x, arXiv:1505.04480.

[38] CMS Collaboration, "Measurement of differential top-quark pair production cross sections in *pp* collisions at $\sqrt{s} = 7$ TeV", *Eur. Phys. J. C* **73** (2013), no. 3, 2339, doi:10.1140/epjc/s10052-013-2339-4, arXiv:1211.2220.

[39] CMS Collaboration, "CMS Luminosity Based on Pixel Cluster Counting - Summer 2013 Update", CMS Physics Analysis Summary CMS-PAS-LUM-13-001, 2013.

[40] CMS Collaboration, "Measurement of the inclusive W and Z production cross sections in pp collisions at $\sqrt{s} = 7$ TeV with the CMS experiment ", *JHEP* **10** (2011) 132, doi:10.1007/JHEP10(2011)132, arXiv:1107.4789.

[41] M. Czakon and A. Mitov, "Top++: A Program for the Calculation of the Top-Pair Cross-Section at Hadron Colliders", *Comput. Phys. Commun.* **185** (2014) 2930, doi:10.1016/j.cpc.2014.06.021, arXiv:1112.5675.

[42] M. Botje et al., "The PDF4LHC Working Group Interim Recommendations", arXiv:1101.0538.

[43] CMS Collaboration, "Measurement of W^+W^- and ZZ production cross sections in pp collisions at $\sqrt{s} = 8$ TeV", *Phys. Lett. B* **721** (2013) 190, doi:10.1016/j.physletb.2013.03.027, arXiv:1301.4698.

[44] S. Alekhin et al., "The PDF4LHC Working Group interim report", (2011). arXiv:1101.0536.

[45] P. M. Nadolsky et al., "Implications of CTEQ global analysis for collider observables", *Phys. Rev. D* **78** (2008) 013004, doi:10.1103/PhysRevD.78.013004, arXiv:0802.0007.

[46] A. D. Martin, W. J. Stirling, R. S. Thorne, and G. Watt, "Update of parton distributions at NNLO", *Phys. Lett. B* **652** (2007) 292, doi:10.1016/j.physletb.2007.07.040.

[47] M. Ubiali, "NNPDF1.0 parton set for the LHC", *Nucl. Phys. Proc. Suppl.* **186** (2009) 62, doi:10.1016/j.nuclphysbps.2008.12.020.

[48] CMS Collaboration, "Determination of Jet Energy Calibration and Transverse Momentum Resolution in CMS", *J. Instrum.* **6** (Jul, 2011) P11002.

[49] R. Barlow and C. Beeston, "Fitting using finite Monte Carlo samples", *Comp. Phys. Comm.* **77** (1993) 219, doi:10.1016/0010-4655(93)90005-W.

[50] A. L. Read, "Presentation of search results: the CL_s technique", *J. Phys. G* **28** (2002) 2693, doi:10.1088/0954-3899/28/10/313.